

Integrated micro/macro-mechanical model of woven fabric composites under large deformation

Pu Xue^a, Jian Cao^{a,*}, Julie Chen^b

^a Department of Mechanical Engineering, Northwestern University, Evanston, IL 60208, USA

^b Department of Mechanical Engineering, University of Massachusetts Lowell, Lowell, MA 01854, USA

Available online 13 September 2004

Abstract

Thermoforming of woven composite panels generally involves significant in-plane shear deformation, and induces additional anisotropy into the composites. In our previous paper, a new constitutive model for macro-mechanically characterizing the non-orthogonal material behavior under large deformation was proposed. In the present work, we develop an integrated micro- and macro-constitutive model to predict the mechanical properties of woven composites during large deformation based on the micro-structure of composites, i.e., the dimensions of fibers, yarns and unit cell, the material properties of composite constituents, as well as the orientation of yarns. The modeling strategy starts with a geometrical description of the yarn and the unit cell during a trellising shear deformation. Following this, a mechanistic analysis on a unit cell has been conducted to determine the equivalent shear properties of woven composites used in our non-orthogonal model. Meanwhile, a simple and conventional analytical technique is applied to predict the tensile properties of woven composites. The proposed integrated micro/macro-model shows excellent agreement with the experimental data and the 3D finite element results. Finally, a parametric study is performed using the presented models to investigate the effects of major geometrical parameters and material properties of the constituents on the shear properties of plain weave composites.

© 2004 Elsevier Ltd. All rights reserved.

Keywords: Woven composite; Micro/macro-constitutive model; Non-orthogonal; Large deformation; Thermoforming; Shear deformation

1. Introduction

Composite panels reinforced by woven fabric are of increasing interest in applications such as aircraft, automobiles and pressure vessels, etc. due to their high strength/weight performance as compared to metal sheets. In addition, they can also offer many advantages including dimensional stability and good conformability to a complex shape. However, manufacturing curved parts generally involves long cycle times and significant manual labor in laying out the woven fabric to the specific tooling geometry. Thermo-stamping from an initial

flat composite sheet offers a potentially cost-effective route for rapidly producing complex-shaped parts.

Thermoforming of woven composite panels generally involves significant in-plane shear deformation, and induces additional anisotropy into the composites. In our previous paper [1], a new constitutive model for characterizing the non-orthogonal material behavior under large deformation was proposed. The model can be used to efficiently predict material responses under various loading paths for woven composites with different weave architectures. Geometric non-linearity and material non-linearity, as well as complex redistribution and reorientation of the warp and weft yarns during deformation were taken into account. The equivalent material properties in the model were determined by fitting the numerical load vs. displacement curves to experimental

* Corresponding author. Tel.: +1 847 491 3915.

E-mail address: jcao@northwestern.edu (J. Cao).

results for two simple cases: biaxial tension and pure shear deformation. The resulting model was then shown to match the experimental results for more complex loading cases. As known, the behavior of composites strongly depends on the geometric and physical parameters of the constituents, i.e. reinforcing fibers and matrix, and the fabric architecture. It is desirable to directly correlate these micromechanical and microstructural parameters to the equivalent material properties used in our phenomenological constitutive equation developed in [1]. With that, we can study the effects of various parameters on the behavior of woven composites, and then efficiently design the weave architecture and tailor the constituents of a woven composite for a specific application.

This complex relationship between the fiber properties and the composite behavior has been explored through many experimental and theoretical studies. Among approaches investigated are the 3D finite element method in conjunction with a micromechanical model [2,3] and the homogenization method [4,5]. These methods can take into account the shape of the cross section and the curvilinear profile of yarns, and account for the geometric and material characteristics associated with the fabric reinforcement and the resin. However, in general, these methods are computationally costly even for simple fiber architectures, and because of this, they have not been effective in optimizing the forming process.

Compared to numerical approaches, analytical methods are much more efficient, although they usually involve various assumptions describing the fabric geometry and determining the mechanical properties of the composite. Most of the existing analytical models were proposed for conventional consolidated composites e.g. [6,7]. These models are only applicable under small deformation. The flexible composites used in thermo-stamping are different from the conventional consolidated composites, with the former possessing much larger potential deformation than the latter. Realf et al. [8] proposed an analytical approach to modeling the fabric behavior under tensile loading conditions, where the original fabric geometry, bending behavior, consolidation response, and flattening response were considered. In forming woven fabrics or flexible composites into complex shapes, however, shear deformation is a dominant mechanism. When the part geometry possesses a double curvature, the forming process usually results in a complex redistribution and reorientation of yarns in the woven fabric reinforced composite. The existing material models addressing these large shear characteristics are very limited. In the following paragraph, the literature in this specific area will be reviewed.

Blanlot and Billoët [9] proposed a mechanical approach, in which material behavior was assumed to

be orthotropic in the frame that coincided with the directions of bisectors of the warp and weft roving, which were not orthogonal to each other after the shear deformation. Their formulation could characterize the evolution of the orthogonal hypoelastic law by updating the location of the bisectors of the warp and weft roving. However, the determination of material properties in the rotating frame needs further investigation. Vu-Khanh and Liu [10] characterized a deformed fabric composite (non-orthogonal architecture) by a laminate composed of four uni-directional plies. Based on the classical laminated plate theory, the stiffness matrices of the sub-ply model were obtained. The effect of fiber undulation could be considered by experimentally measuring the equivalent elastic coefficients of the constituent plies. Both approaches i.e. [9,10] considered the non-orthogonal properties in their models, however, they did not correlate the geometry and material parameters of the constituents and the fabric architecture to the material properties of the composite. Harrison et al. [11] presented two shear models for woven composites based on the fiber diameter, fiber volume fraction, weave type and matrix viscosity. McBride and Chen [12], Bulusu and Chen [13] proposed their geometric unit cell models to study the evolution of the yarn geometry and fabric architecture during pure shear deformation. The parameters of yarns and unit cell and the yarn orientation, θ , were incorporated in the geometric models. They assumed that yarns rotated about interlacing points, neglecting the yarn extension. These authors are probably the first ones who tried to model the yarn deformation to predict forming behavior due to shearing within tow and inter-tow region, as well as between tow cross-overs. Their models can serve as an important guide to further modeling. Following this technique route, Yu et al. [14] presented a nonorthogonal constitutive model by considering microstructures of composites. At the current stage, more investigation is needed.

This paper aims to develop an integrated micro/macro-constitutive model to predict the behavior of woven composites during large deformation based on the geometric parameters of fibers, yarns and unit cell, the material constants of composite constituents, and the orientation of yarns. The modeling strategy starts with a geometric description of the yarn and the unit cell during the trellising shear deformation. Then, the mechanistic analysis on the unit cell has been carried out to obtain the stiffness and the compliance matrices associated with the geometric model, followed by the determination of the equivalent shear properties to be used in our previous non-orthogonal model [1]. Meanwhile, a simple and conventional analytical technique, combining the classical rule of mixtures of unidirectional composites, is used to predict the tensile properties of woven composites. The results predicted by this model are compared with those obtained from the experimen-

tal data or 3D finite element numerical simulations. Finally, a parametric study is performed to investigate the effects of major geometric parameters of the fabric architecture and material properties of the constituents on the shear properties of plain weave composites.

2. Geometric and physical description of the unit cell under trellising shear deformation

For a woven fabric, warp and weft yarns are interlaced. Typical weave patterns includes balanced plain weave, imbalanced plain weave, 2 × 2 twill and satin weaves. A *balanced plain weave* shown in Fig. 1(a), whose physical and geometric properties are identical in the warp and weft directions, is the simplest fabric architecture. This pattern can provide uniform strength in the two yarn directions.

The mechanical behavior of woven composites is highly dependent upon the geometric and physical parameters of the yarns and the reinforcing fabric. This section will relate the trellising shear deformation to the geometric and physical description of the balanced plain weave composite based on McBride and Chen’s model [12,15], in which a micromechanical unit cell model for plain weave was presented and its evolutions of the microstructures during large shear deformation were described. Improvement made in this paper is the development of the yarn compaction model. The methodology used in this section is not only suitable for the plain weave, but for the other woven structures. For the latter, geometric descriptions of yarns and a unit cell need to be modified correspondingly.

2.1. Geometric description of plain weave architecture

The basic repeating unit, i.e. the unit cell, of balanced plain weave is isolated in Fig. 1(b). From photomicro-

graphs of the woven fabric, the yarn path can be assumed to be approximately sinusoidal provided that the side length of the unit cell, s , the yarn width, w , inter-yarn gap, $g = s - w$, fabric thickness, h , and the undulation of the yarn expressed by the parameter, U , are known, as shown in Fig. 1(c). For a balanced plain weave pattern, $U = h$, which is used for the demonstration purpose in this section. The parameter, s , will reduce to w if no gap is considered. Let y_1 and y_2 be the top and the bottom sinusoidal paths of the warp yarn, and y_3 and y_4 be the bottom and the top segments of the two adjacent weft yarns, respectively. Then, the yarn’s paths can be expressed in terms of the yarn and unit cell geometric parameters as

$$\begin{aligned}
 y_1(x) &= \frac{h}{2} \left(\cos \frac{\pi x}{s} + 1 \right) & 0 \leq x \leq s \\
 y_2(x) &= \frac{h}{2} \left(\cos \frac{\pi x}{s} - 1 \right) & 0 \leq x \leq s \\
 y_3(x) &= -h \cos \left(\frac{\pi x}{s_1} \right) & 0 \leq x \leq w/2 \\
 y_4(x) &= -h \cos \frac{\pi [x - (s - s_1)]}{s_1} & (s - w/2) \leq x \leq s
 \end{aligned}
 \tag{1}$$

The geometric parameter s_1 , the half period of the function y_3 , can be determined by equating $y_3(x = w/2)$ with $y_2(x = w/2)$, then

$$s_1 = \frac{\pi w}{2 \cos^{-1} \left[\sin^2 \left(\frac{\pi w}{4s} \right) \right]}
 \tag{2}$$

which is related to the crimp of the fabric.

Note that a tensile force is applied to warp yarns during the weaving process, and the undulation of the warp yarns determines the cross-sectional shape of the weft yarns, and vice versa. In this model, it is assumed that the shape and the area of the cross section keep unchanged along the yarn direction. The cross-sectional area of a yarn, A (the shaded area in a unit cell, Fig.

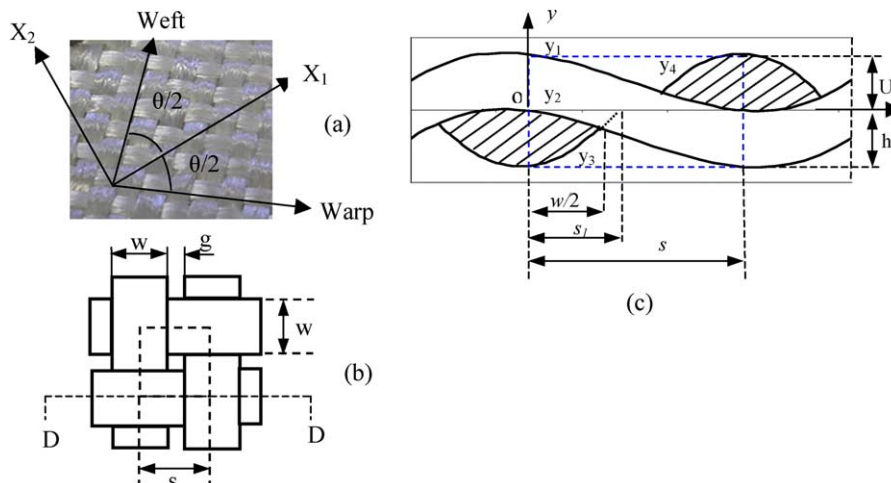


Fig. 1. (a) Balanced plain weave; (b) unit cell; (c) cross-section D – D of the unit cell.

1(c)), and the length of a yarn in the unit cell, L , can be calculated, respectively, by

$$A = 2 \int_0^{w/2} |y_3(x) - y_2(x)| dx \quad (3)$$

$$L = \int_0^s \left(\sqrt{1 + \left[\frac{dy_1(x)}{dx} \right]^2} \right) dx \quad (4)$$

The fiber volume fraction of a yarn is then given by

$$V_f = \frac{\text{fiber volume}}{\text{yarn volume}} = \frac{\pi D^2 N}{4A} \quad (5)$$

where the diameter of the fiber, D , and the number of fibers in a yarn, N , are provided by suppliers.

During the trellising shear deformation, the angle between the weft and warp yarns, θ , will change, then the yarn width, w , and the half period of the function y_3 , s_1 , as well as y_3 and y_4 all vary with the shear deformation. This will lead to changes in the cross-sectional area (A) and the fiber volume fraction (V_f) of a yarn.

2.2. Yarn compaction model

Considering that the warp and weft yarns in a woven fabric are interlaced, the two sets of the yarns compact one another, resulting in the change of the yarn width with the increase of trellising deformation. The variation of the yarn width depends on the microstructure of the woven composites. Based on the measurements, the yarn width, w , can be assumed to vary with the shear deformation by

$$w = w_0 (\sin \theta)^{\alpha g_0 / w_0} \quad (6)$$

where w_0 and g_0 are the initial yarn width and inter-yarn gap, respectively. α is an adjustable coefficient. For the fabric considered in this paper, $w_0 = 3.72$ mm and $g_0 = 1.42$ mm. α is determined as 1.2 to make the assumed compaction model match the experimental measurement well. It was proposed [12] that the quantity of $[(s - w)/s_1]$ can be used as a measurement of fabric tightness. Fig. 2 demonstrated the measured result for woven fabrics with the fabric tightness equal to 0.23. The yarn width normalized by the initial value is plotted vs. the angle. It was shown that the yarn width decreases during the trellising deformation. θ . For the fabric considered in this paper the fabric tightness equals to 0.24, similar to that used in the measurement. It can be seen that Eq. (6) can represent the yarn compaction well.

Eqs. (1)–(6) give the continuous geometric description of the unit cell during the trellising deformation. Using the above method for geometric modeling, the size and the spatial orientation of a yarn in the woven fabric network have been fully identified during the shear deformation.

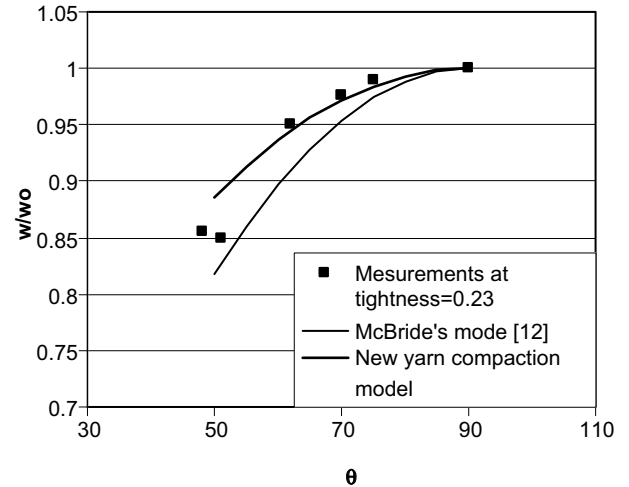


Fig. 2. Comparison of yarn compaction models.

2.3. Micromechanical analysis of a yarn and a unit cell

Suppose a fabric lies in the X_1 – X_2 plane, as shown in Fig. 3, with the X_1 axis bisecting the angle between the warp and weft yarns. The weft yarn can be discretized by vertical slices normal to the X_1 – X_2 plane. The local orthogonal coordinate system (x_i'') can be defined. The x_1'' axis is along the tangent of yarn's centerline. The x_2'' axis is always parallel to the X_1 – X_2 plane. The angles defining the orientation of the n th slice are $\theta/2$ and, as shown in Fig. 3.

Yarns can be treated as a continuum because the inter-fiber gap is small compared to the cross-sectional size of the yarn. Each slice is assumed to be transversely isotropic (isotropic in the x_2'' – x_3'' plane) and the stress and strain are assumed to be uniform within a given slice. Therefore, its constitutive equation in the coordinate system (x_i'') can be written as:

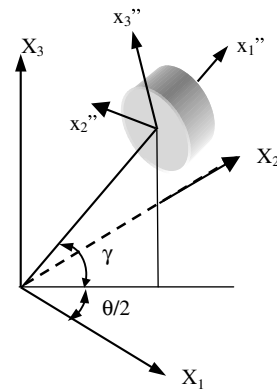


Fig. 3. Yarn's discretization and orientation in the global and the local coordinates.

$$\begin{Bmatrix} d\varepsilon_1 \\ d\varepsilon_2 \\ d\varepsilon_3 \\ d\varepsilon_{12} \\ d\varepsilon_{23} \\ d\varepsilon_{13} \end{Bmatrix}_n'' = \begin{bmatrix} S_{11} & S_{12} & S_{12} & & & \\ S_{12} & S_{22} & S_{23} & & & \\ S_{12} & S_{23} & S_{22} & & & \\ & & & S_{66} & & \\ & & & & S_{55} & \\ & & & & & S_{66} \end{bmatrix}_n \begin{Bmatrix} d\sigma_1 \\ d\sigma_2 \\ d\sigma_3 \\ d\sigma_{12} \\ d\sigma_{23} \\ d\sigma_{13} \end{Bmatrix}_n'' \quad (7)$$

or

$$d\varepsilon_n'' = S_n d\sigma_n''$$

where the subscript n corresponds to the n th slice. The compliance matrix S depends on the level of the shear deformation. Based on the mechanistic analysis [15], each element in Eq. (7) can be determined as

$$S_{11} \approx \frac{4V_a}{\pi E V_f} \quad (8)$$

$$S_{22} = \frac{\frac{\beta_1^4}{3\pi E} \left(\sqrt{\frac{V_a}{V_f}} - 1\right)^5}{\sqrt{\frac{V_a}{V_f}} \left(5 - \sqrt{\frac{V_f}{V_a}} - 4\sqrt{\frac{V_0}{V_f}}\right)} \quad (9)$$

$$S_{12} = \frac{-16\beta_1^2}{\pi^3 E} \times \sqrt{\frac{V_a}{V_f}} \left(\sqrt{\frac{V_a}{V_f}} - 1\right)^3 \left[1 - \frac{\left(1 - \sqrt{\frac{V_f}{V_0}}\right) \left(4\sqrt{\frac{V_a}{V_f}} - 1\right)}{\left(4\sqrt{\frac{V_a}{V_f}} - 5\sqrt{\frac{V_a}{V_0}} + \sqrt{\frac{V_f}{V_0}}\right)}\right] \quad (10)$$

$$S_{23} = -\nu_t S_{22} \quad (11)$$

$$S_{55} = 2(S_{22} - S_{23}) \quad (12)$$

$$S_{66} = \beta_2 S_{55} \quad (13)$$

In the above equations, V_f denotes the current fiber volume fraction as a function of θ calculated from Eq. (5), and V_a and V_0 are the maximum fiber volume fraction, corresponding to a limiting compressibility of aligned fiber yarn, and the initial fiber volume fraction, respectively. E is the Young's modulus of the yarn. The transverse Poisson's ratio, ν_t , can be obtained from a compression experiment. The geometric parameter, β_1 is defined as the ratio of the wavelength to the amplitude of the sinusoidal curve of the yarn, which is related to the undulation of the fabric. It was reported in [15,16] that the value of β_1 ranges from 64 to 280 for resin impregnated fiber bundles. The transverse shear compliance, S_{66} , is assumed to be proportional to the in-plane shear compliance, S_{55} and β_2 denotes the proportional coefficient. The value of $\beta_2 = 2$ was suggested in [15]. The inversion of the compliance matrix gives the stiffness matrix, i.e.

$$d\sigma_n'' = S_n^{-1} d\varepsilon_n'' = C_n d\varepsilon_n'' \quad (14)$$

This constitutive equation, in the local coordinate system, can be transferred to that in the global system. The strain and stress in the global and the local coordinate systems are related by the following equations:

$$\varepsilon_n'' = T_1 \varepsilon, \quad \sigma = T_1^T \sigma'' \quad (15)$$

where

$$T_1 = \begin{bmatrix} l_1^2 & m_1^2 & n_1^2 & l_1 m_1 & m_1 n_1 & n_1 l_1 \\ l_2^2 & m_2^2 & n_2^2 & l_2 m_2 & m_2 n_2 & n_2 l_2 \\ l_3^2 & m_3^2 & n_3^2 & l_3 m_3 & m_3 n_3 & n_3 l_3 \\ 2l_1 l_2 & 2m_1 m_2 & 2n_1 n_2 & l_1 m_2 + m_1 l_2 & m_1 n_2 + n_1 m_2 & l_1 n_2 + n_1 l_2 \\ 2l_2 l_3 & 2m_2 m_3 & 2n_2 n_3 & l_2 m_3 + m_2 l_3 & m_2 n_3 + n_2 m_3 & l_2 n_3 + n_2 l_3 \\ 2l_1 l_3 & 2m_1 m_3 & 2n_1 n_3 & l_1 m_3 + m_1 l_3 & m_1 n_3 + n_1 m_3 & l_1 n_3 + n_1 l_3 \end{bmatrix}$$

l_i , m_i and n_i ($i = 1, 2, 3$) are the direction cosines of unit vectors in the local coordinate, i.e.

$$\begin{bmatrix} i'' \\ j'' \\ k'' \end{bmatrix} = \begin{bmatrix} l_1 & m_1 & n_1 \\ l_2 & m_2 & n_2 \\ l_3 & m_3 & n_3 \end{bmatrix} \begin{bmatrix} i \\ j \\ k \end{bmatrix} = \begin{bmatrix} \cos \frac{\theta}{2} \cos \gamma & \sin \frac{\theta}{2} \cos \gamma & \sin \gamma \\ -\sin \frac{\theta}{2} & \cos \frac{\theta}{2} & 0 \\ -\cos \frac{\theta}{2} \sin \gamma & -\sin \frac{\theta}{2} \sin \gamma & \cos \gamma \end{bmatrix} \begin{bmatrix} i \\ j \\ k \end{bmatrix}$$

Therefore, with respect to the global coordinate system, the relationship between the stress and strain increments of the n th slice can be obtained as

$$d\sigma_n = (T_1^T C T_1)_n d\varepsilon_n \quad (16)$$

Then the average stress increment in the unit cell

$$d\sigma = \sum_{n=1}^M (\phi_n T_1^T C T_1)_n d\varepsilon \quad (17)$$

where ϕ_n is the volume ratio of the n th slice to the unit cell. M is total number of the yarn sections in a unit cell. For a plain woven structure, M is equal to four times the number of slices in a single yarn. Thus, the instantaneous average fabric properties under the large shear deformation are given by

$$C_{\text{sum}} = \sum_{n=1}^M \phi_n (T_1^T C T_1)_n \quad (18)$$

Eq. (17) gives the relationship between the stresses and the strains in the global system. T_1 and C_n all depend upon the level of the trellising deformation.

Up to this point, the micromechanical unit cell model for plain weave fabric reinforced composites have been fully determined by the geometry and material properties of the constituents and the fabric architecture. The major geometric parameters include the known parameters, i.e. the diameter of the fiber, D , the number of the fibers in a yarn, N , the number of yarns in a unit cell, and the initially measured parameters, like the yarn

width, w , the yarn gap, g , and the thickness of the fabric, h . The geometry and the mechanical behavior both are dependent of the level of the trellising deformation, represented by θ .

3. A non-orthogonal constitutive model for characterizing woven composites under large deformation

In order to effectively characterize woven composites, equivalent shell elements are used to model the woven composite panel. In this section, we will first summarize the relationship between stresses and strains in the new constitutive law [1], then demonstrate how to determine the material properties used in the non-orthogonal model, based on the microstructure and the material constants of the constituents and the unit-cell.

3.1. Relationship between stresses and strains

In the following derivation, three sets of coordinates are selected on the middle surface of a woven composite. They are the global coordinate system OXY , the local coordinate system $O'X'Y'$ in which the axis X' coincides with the current warp direction of the fabric, and the material coordinate system $O'\xi\eta$, where ξ and η are chosen to coincide with the current warp and weft directions of the fabric, respectively. The axes ξ and η are orthogonal to each other in the original configuration, but will become non-orthogonal after shear deformation occurs, as shown in Fig. 4.

Since $O'\xi\eta$ is in non-orthogonal coordinates, the complementary property of shear stresses does not necessarily hold. Instead, two shear stress components, $\tau_{\xi\eta}$ and $\tau_{\eta\xi}$, need to be introduced. Therefore, the stress state in the non-orthogonal coordinate system $O'\xi\eta$ can be expressed by four components, which are:

$$[\sigma_{\xi} \quad \sigma_{\eta} \quad \tau_{\xi\eta} \quad \tau_{\eta\xi}]^T$$

Based on the force equilibrium, it can be obtained such that

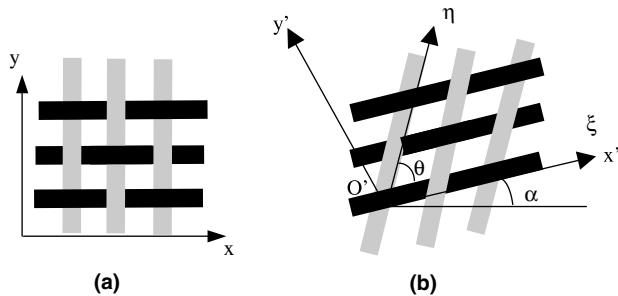


Fig. 4. Schematic of a woven structure: (a) before deformation; (b) after shear deformation.

$$\begin{aligned} \begin{bmatrix} \sigma_{x'} \\ \sigma_{y'} \\ \tau_{x'y'} \end{bmatrix} &= \begin{bmatrix} 1 & 0 & 0 & 0 \\ 0 & 1 & -\cot\theta & -\cot\theta \\ -\cot\theta & \cot\theta & 0 & 1 \end{bmatrix} \begin{bmatrix} \sigma_{\xi} \\ \sigma_{\eta} \\ \tau_{\xi\eta} \\ \tau_{\eta\xi} \end{bmatrix} \\ &= T_2 \begin{bmatrix} \sigma_{\xi} \\ \sigma_{\eta} \\ \tau_{\xi\eta} \\ \tau_{\eta\xi} \end{bmatrix} \end{aligned} \quad (19)$$

where T_2 is a 3×4 transformation matrix for the stress components from the non-orthogonal coordinates $O'\xi\eta$ to the orthogonal coordinates $O'X'Y'$. $\sigma_{x'}$, $\sigma_{y'}$ and $\tau_{x'y'}$ are stress components in the $O'X'Y'$ coordinates.

Correspondingly, it is also necessary to introduce four strain components in the local non-orthogonal coordinates, which are

$$[\epsilon_{\xi} \quad \epsilon_{\eta} \quad \gamma_{\xi\eta} \quad \gamma_{\eta\xi}]^T$$

where ϵ_{ξ} and ϵ_{η} are the normal strains along the warp and the weft directions, respectively. $\gamma_{\xi\eta}$ and $\gamma_{\eta\xi}$ are the shear strains reflecting the angular change from a right angle formed by axes ξ and η at the initial position, and $\gamma_{\eta\xi} = \gamma_{\xi\eta}$. Based on the strain analysis, we have

$$\begin{aligned} \begin{bmatrix} \epsilon_{\xi} \\ \epsilon_{\eta} \\ \gamma_{\xi\eta} \\ \gamma_{\eta\xi} \end{bmatrix} &= \begin{bmatrix} 1 & 0 & 0 \\ \cos^2\theta & \sin^2\theta & \sin\theta\cos\theta \\ 0 & 0 & 1 \\ 0 & 0 & 1 \end{bmatrix} \begin{bmatrix} \epsilon_{x'} \\ \epsilon_{y'} \\ \gamma_{x'y'} \end{bmatrix} \\ &= T_3 \begin{bmatrix} \epsilon_{x'} \\ \epsilon_{y'} \\ \gamma_{x'y'} \end{bmatrix} \end{aligned} \quad (20)$$

where T_3 is a 4×3 transformation matrix connecting the strain components between $O'\xi\eta$ and $O'X'Y'$.

It has been verified experimentally in the biaxial tensile test by Boisse's group [17] that the shear stresses and strains and the normal stresses and strains can be treated as uncoupled in the material coordinates $O'\xi\eta$. Therefore, the relationship between stress and strain components for woven composites can be approximately expressed as

$$\begin{aligned} \begin{bmatrix} \sigma_{\xi} \\ \sigma_{\eta} \\ \tau_{\xi\eta} \\ \tau_{\eta\xi} \end{bmatrix} &= \begin{bmatrix} D_{11} & D_{12} & 0 & 0 \\ D_{21} & D_{22} & 0 & 0 \\ 0 & 0 & \beta_3 D_{33} & 0 \\ 0 & 0 & 0 & (2 - \beta_3) D_{33} \end{bmatrix} \begin{bmatrix} \epsilon_{\xi} \\ \epsilon_{\eta} \\ \gamma_{\xi\eta} \\ \gamma_{\eta\xi} \end{bmatrix} \\ &= D \begin{bmatrix} \epsilon_{\xi} \\ \epsilon_{\eta} \\ \gamma_{\xi\eta} \\ \gamma_{\eta\xi} \end{bmatrix} \end{aligned} \quad (21)$$

where β_3 is a coefficient that stands for the contribution to the total shear property from each shear stress. For

balanced plain weave, $\beta_3 = 1$. D is a material matrix in the coordinate system $O'\zeta\eta$. D_{11} , D_{12} , D_{21} and D_{22} describe the tensile properties of the woven composite and can be described as functions of an equivalent strain defined as

$$\bar{\varepsilon}^+ = \frac{2}{\sqrt{3}} \sqrt{(\varepsilon_1^+)^2 + (\varepsilon_2^+)^2 + (\varepsilon_1^+)(\varepsilon_2^+)} \quad (22)$$

Since flexible woven composites cannot effectively sustain compressive load, the negative strain(s) would not contribute to the load-carrying capability of the material. In this consideration, ε_1^+ and ε_2^+ in Eq. (22) are normal tensile strains along each yarn direction. The element D_{33} denotes the shear property of the material and can be assumed as a function of the shear strain. Combining Eqs. (19)–(21), the relationship between the stress and strain components in the coordinate system $O'X'Y'$ can be expressed as

$$\sigma_{x'y'} = T_2 \cdot D \cdot T_3 \varepsilon_{x'y'} = \bar{D} \varepsilon_{x'y'} \quad (23)$$

After transforming from the coordinate system $O'X'Y'$ to OXY , the constitutive equation of woven composites under large deformation can be found as

$$\begin{bmatrix} \sigma_x \\ \sigma_y \\ \tau_{xy} \end{bmatrix} = R \bar{D} R^T \begin{bmatrix} \varepsilon_x \\ \varepsilon_y \\ \gamma_{xy} \end{bmatrix} = R T_2 D T_3 R^T \begin{bmatrix} \varepsilon_x \\ \varepsilon_y \\ \gamma_{xy} \end{bmatrix} \quad (24)$$

where R is the unit transformation matrix between the local orthogonal coordinates $O'X'Y'$ and the global orthogonal coordinates OXY , and can be expressed as

$$R = \begin{bmatrix} \cos^2 \alpha & \sin^2 \alpha & -2 \sin \alpha \cos \alpha \\ \sin^2 \alpha & \cos^2 \alpha & 2 \sin \alpha \cos \alpha \\ \sin \alpha \cos \alpha & -\sin \alpha \cos \alpha & \cos^2 \alpha - \sin^2 \alpha \end{bmatrix} \quad (25)$$

Based on the above equations, the stress state of the woven composite in the global coordinate system OXY can be obtained for a given strain state.

3.2. Integration of the micro- and macro-models

In this subsection, we will first illustrate how to determine the shear properties (D_{33} in Eq. (21)), followed by the determination of the tensile property (D_{11} , D_{12} , D_{21} , D_{22} , in Eq. (21)).

3.2.1. Shear properties

Eq. (17) provides the relationship between the stress and strain matrices in the coordinate system, $OX_1X_2X_3$ (Fig. 1a), while the constitutive equation Eq. (24) characterizes the material behavior in the global coordinate system $OXYZ$. After transferring Eq. (17) to the global system $OXYZ$ and matching the obtained equations with Eq. (24), the equivalent shear property of the composite material for the shell element, D_{33} in the non-

orthogonal model, can be obtained from the present model.

3.2.2. Tensile properties

In theory, the other elements D_{11} , D_{12} and D_{22} in the constitutive equation (24) can also be obtained in the same way as for D_{33} , as long as the geometric model involves the tensile and trellising shear deformation modes. However, from the previous studies [1], it was understood that the woven composites behave non-linearly only at the initial stage (typically <0.2%) of the tensile test. After the initial nonlinear range, the material behaves almost linearly, similar to that of the yarn alone, except for a greater shrinkage in the direction perpendicular to the loading direction. Therefore, the classical rule of mixtures of unidirectional composite and a simple and straightforward analytical technique can be applied to approximately determine the tensile properties of woven composites. In the following, we will start from determining yarn properties, followed by the properties of the unit cell; and finally, generate the properties of the equivalent shell element.

The tension properties of a composite material depend on the properties of the constituents and their contributions. The longitudinal stiffness of a unidirectional composite yarn can be predicted [18] by

$$E_1 = E_f V_{fp} + E_m (1 - V_{fp}) \quad (26)$$

where V_{fp} is the fiber packing fraction in a yarn. This equation indicates that the contributions of the fiber and the matrix to the average composite properties are proportional to their volume fractions. The prediction of transverse modulus by the Halpin Tsai equation [19] is

$$E_2 = \frac{(1 + \xi \eta V_{fp}) E_m}{1 - \eta V_{fp}} \quad (27)$$

where $\eta = \frac{(E_f/E_m) - 1}{(E_f/E_m) + \xi}$, and is a measure of reinforcement that depends on the fiber geometry, packing geometry, and loading conditions. The value of $\xi = 2$ has been suggested for fibers with a circular or square cross section.

Major and minor Poisson's ratios of a composite with unidirectional fibers reinforced can be expressed as the functions of the fiber packing fraction, the Poisson's ratios and the Young's moduli of the fiber and the matrix [18], i.e.

$$\nu_{12} = \nu_f V_{fp} + \nu_m (1 - V_{fp}) \quad (28)$$

$$\nu_{21} = \nu_{12} \frac{E_2}{E_1} \quad (29)$$

From Eqs. (26)–(29), the Young's modulus of the yarn along the longitudinal and the transverse directions, as well as the Poisson's ratios can be obtained.

Then, tensile properties of the unit cell in the elastic range can be approximately determined by

$$D_{11,u}^e = \frac{\beta_4 E_1}{1 - \nu_{12}\nu_{21}} \quad (30)$$

$$D_{12,u}^e = \frac{\beta_4 \nu_{12} E_2}{1 - \nu_{12}\nu_{21}} \quad (31)$$

The adjustable coefficient β_4 is introduced to reflect the effect of yarns normal to the loading direction on the tensile properties. It depends on the undulation of the yarn in weave architecture. β_4 could be determined by an uniaxial tensile test for woven composite. Usually, it ranges from 1 to 1.2.

Our objective is to determine the equivalent tensile properties in the constitutive equation (24) from the microstructure of the woven composite and the material properties of composite constituents. Because the load vs. displacement curves of the unit cell and the shell element are supposed to be the same under uni-axial tension, and the cross-sectional areas of the yarn and the shell element are A_y and A_s , respectively, then the equivalent tensile stiffness of the material for the shell element within the elastic range can be determined by

$$D_{11,s}^e = D_{11,u}^e \frac{A_y}{A_s} \quad (32)$$

$$D_{12,s}^e = D_{12,u}^e \frac{A_y}{A_s} \quad (33)$$

where the subscript, s, denotes shell element; u and y correspond to unit cell and yarn, respectively.

Within the initial non-elastic range, the main deformation mechanisms are linked to uncrimping of the

yarns under tensile loading. This leads to the nonlinear behavior, which is related to the geometric parameters of the fabric architecture and the imposed strain ratio. Based on our previous study [1], it was known that the tensile stiffness of the material, D_{11} , will increase gradually and approach a constant. Therefore, the tensile stiffness along the loading direction can be expressed as a function of the geometric parameters of the fabric architecture and the equivalent strain as follows:

$$D_{11} = \frac{D_{11,s}^e}{1 + e^{f\epsilon}} \quad (34)$$

where f is a function of the microstructure parameters, such as yarn undulation, yarn thickness, yarn width and inter-yarn gap in a unit cell. The function f describes the effect of the weave architecture on the non-linear tensile property. For the plain weave structure studied, $f = -\frac{(w_0+g_0)^2}{Uh^{3/2}}$ where U is the yarn undulation, h the yarn thickness, w_0 the initial yarn width and g_0 the initial inter-yarn gap between adjacent parallel yarns. D_{11} will approach $D_{11,s}^e$ with the increase of the deformation. Eq. (34) is suitable for the entire deformation process, including the initial non-linear stage and the linear stage afterwards. The function D_{12} , which is determined by Eqs. (31) and (33), can be taken as a constant during the deformation process.

The whole procedure for determining the material parameters described in this section is summarized in Fig. 5.

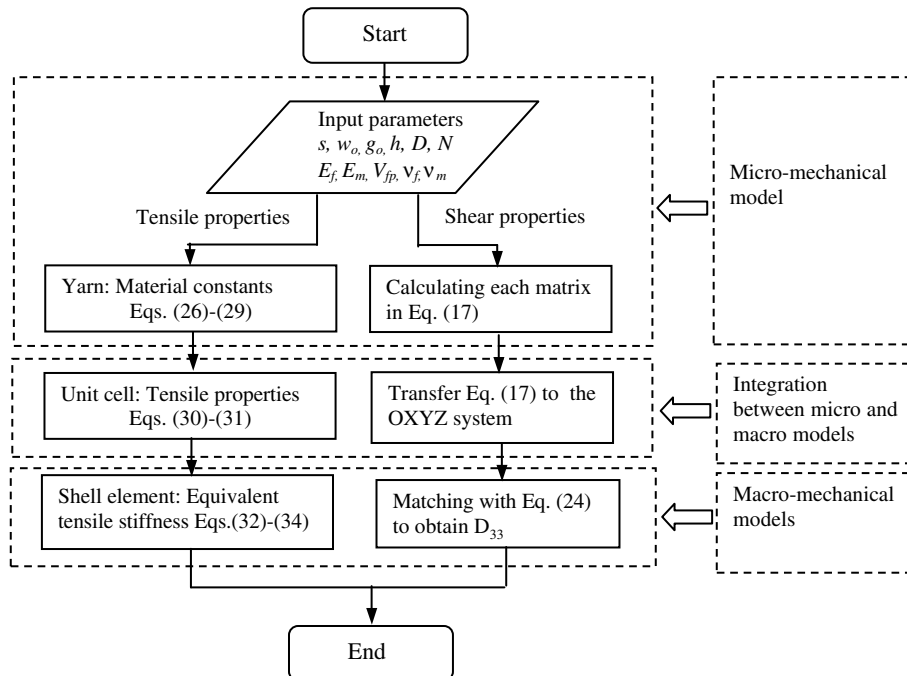


Fig. 5. Flow chart for the determination of material properties.

4. Validation of the proposed model

In order to validate the proposed model, a composite patch with balanced plain-weave fabric reinforcement, subjected to equal biaxial tension, is considered. The geometry of the unit cell is measured as $w = 3.72$ mm, $s = 5.14$ mm, $h = 0.39$ mm and $g = 1.42$ mm. The yarns consist of glass and polypropylene (PP) fibers with a fiber packing fraction in the yarn equal to 0.7. After thermoforming, the glass fibers will act as the reinforcement, while PP fibers will act as the matrix. The material constants of the glass and PP fibers are given in Table 1. Following the procedure illustrated in Fig. 5, for the woven structure considered, the tensile properties of the woven composite can be predicted and listed in Table 2.

After obtaining the equivalent tensile stiffness, the finite element simulation using shell element is conducted by using commercial finite element software (ABAQUS/Standard) incorporated with the obtained material properties. The resulting force vs. displacement curve is presented in Fig. 6 and compared with the numerical result from the 3D unit cell under biaxial tension, showing excellent agreement.

By the procedure described in Fig. 5, in which $\beta_1 = 232$, $\beta_2 = 2$, $V_a = 0.85$ and $\beta_3 = 1$, the shear function, D_{33} , can be expressed as

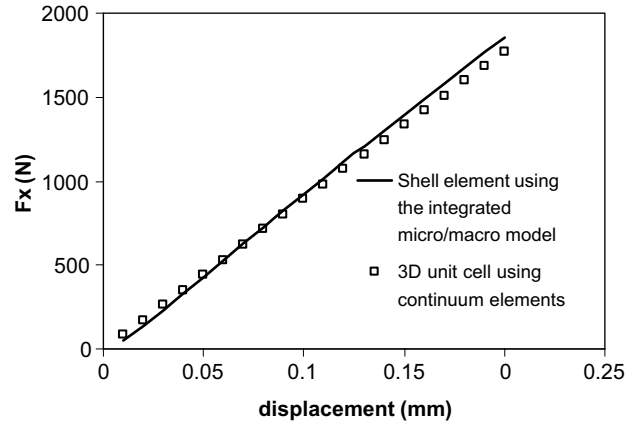


Fig. 6. Comparison of force vs. displacement curve obtained from the proposed integrated model and the 3D unit-cell numerical simulation.

$$D_{33} = 258.48\gamma^6 - 458.61\gamma^5 + 333.43\gamma^4 - 109.15\gamma^3 + 20.04\gamma^2 - 1.01\gamma + 0.012 \text{ (MPa)}$$

In order to compare our predicted results with the experimental data [20], a woven composite patch with the same size (210 mm × 210 mm) as that of the tested sample is considered. The warp and weft yarns are parallel to the edges of the patch. The patch is discretized by 10 × 10 identical shell elements (element type S4R in ABAQUS). Boundary conditions are prescribed to reflect the behavior of the experimental trellising shear frame; that is, the four edges of the composite patch can only rotate rigidly around the corner points. An increasing displacement is imposed along the diagonal direction of the patch. Using a commercial finite element package (ABAQUS/Standard) incorporated with the obtained material properties, the reaction force and the end nodal displacement are recorded, as shown in Fig. 7. Comparing the numerical result with the experimental data obtained at room temperature, a reasonable agreement is attained.

Table 1
Material constants of the glass fiber and PP fiber

Property	Unit	E-glass	PP
Axial modulus	GPa	73.1	3.45
Transverse modulus	GPa	73.1	3.45
Axial Poisson's ratio	–	0.22	0.35
Transverse Poisson's ratio	–	0.22	0.35
Shear modulus	GPa	30.19	1.83
Density	kg/m ³	2540	900

Table 2
Tensile property of the woven composite studied

Tensile properties of the composite	
Yarn	$E_1 = 52.2$ GPa $E_2 = 19.57$ GPa $\nu_{12} = 0.259$ $\nu_{21} = 0.097$
Unit cell	$\beta_4 = 1.08$ $D_{11,u}^e = 57.83$ GPa $D_{12,u}^e = 2.10$ GPa
Shell element	$f = -278.14$ $\beta_3 = 1$ $D_{11} = \frac{12.60}{1+e^{-278.14\epsilon}}$ GPa $D_{12} = 460$ MPa $D_{21} = D_{12}$ $D_{22} = D_{11}$

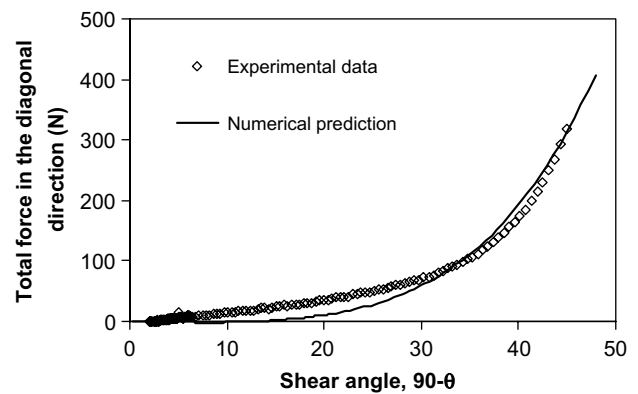


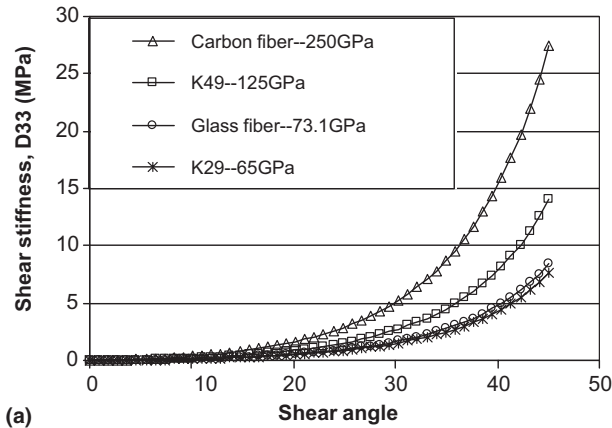
Fig. 7. Comparison of total force obtained from the experiment data [20] and the proposed integrated model.

5. Parametric study

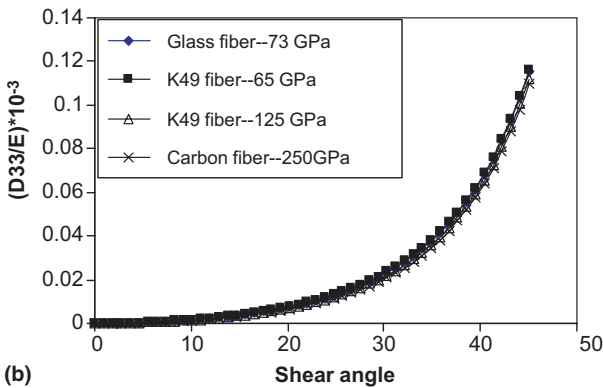
In this section, we will discuss the effects of major geometric parameters, material constants and fiber packing fraction of the yarn on the shear property of a plain weave composite by using the presented integrated micro/macro-mechanical model, so as to provide constructive conclusions for engineering applications.

Figs. 8–10 examine the effects of three parameters on the shear property of woven composites, i.e. the Young’s modulus of the reinforced fibers, the fiber packing fraction, and the yarn gap size of the plain weave architecture. The reinforced fibers considered here are Kevlar fiber K29, glass fiber, Kevlar fibers K49 and carbon fiber, with Young’s moduli of 65 GPa, 73 GPa, 125 GPa and 250 GPa, respectively. The fiber packing fraction, V_{fp} , varies from 0.5 to 0.8. The yarn gap between adjacent parallel yarns changes from 0.5 mm to 2 mm for a constant yarn width of 3.72 mm. It is clear that the shear stiffness of woven composites is closely related to the material properties of the composite constituents and the architecture of woven fabric.

Fig. 8 shows that the Young’s modulus of the reinforced fiber has a positive effect on the shear stiffness.



(a)



(b)

Fig. 8. Effect of the Young’s modulus of the fibers on predicted shear property of the woven composite: (a) D_{33} ; (b) D_{33} normalized by Young’s modulus of the fibers.

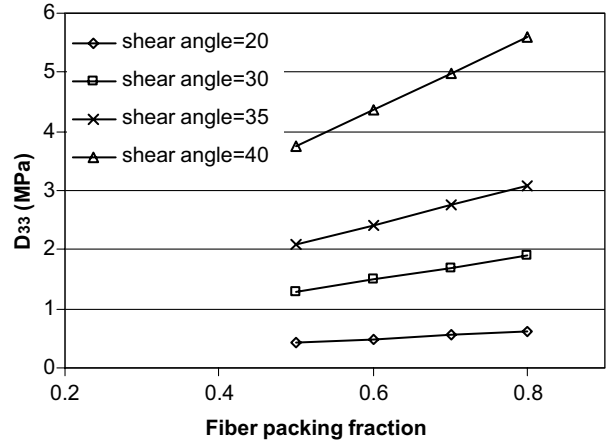


Fig. 9. Effect of fiber packing fraction on shear property of the woven composite.

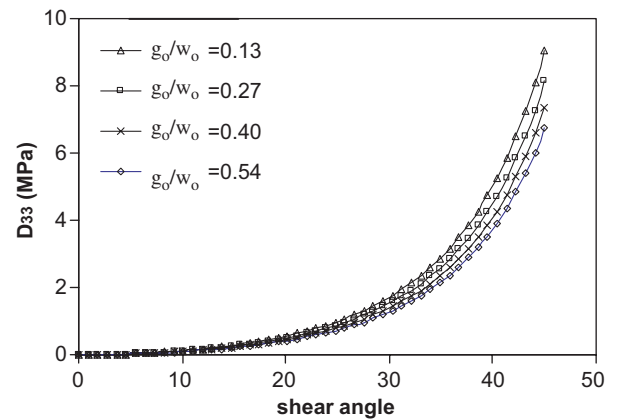


Fig. 10. Effect of the yarn gap of plain weave architecture on shear property of the woven composite.

Carbon fiber, with the highest Young’s modulus, causes the composite to possess more resistance in shear deformation. Note that early shear is insensitive to the Young’s modulus, E , until the shear angle reaches about 20° and the yarns start to compact. After being normalized by the Young’s modulus of the reinforced fiber, it is found that all the curves become very close, as shown in Fig. 8(b). Therefore, the shear stiffness of the woven composite is proportional to the Young’s modulus of the reinforced fiber.

Fig. 9 shows that increasing fiber packing fraction of the yarn, V_{fp} , will enhance the shear stiffness, and the relative percentage of the enhancement varies with the amount of shear deformation in woven composites. At a higher shear deformation, the effect of the fiber packing fraction is more apparent. When the fiber packing fraction varies from 0.5 to 0.8, the impact of the fiber packing fraction is linear on the shear property of the woven composite under a given level of shear deformation.

From Fig. 10 it can be concluded that a larger inter-yarn gap between two adjacent parallel yarns will make the fabric looser, resulting in a lower shear stiffness of the woven composite. However, for the material system studied here, this phenomenon becomes obvious only when the shear deformation is larger than 30° when the yarns start to compact each other. Smaller yarn gaps will introduce shear locking at an earlier stage.

6. Conclusions

An integrated micro/macro-model is developed in the present paper for woven fabric composites under combined tensile and large shear deformation. The framework of the approach consists of the geometric model of yarns and a unit cell, and the non-orthogonal constitutive equations under large deformation, which is shown in Fig. 5. As all the other analytical models, some assumptions are made:

- shape and the area of the cross section are the same along the yarn direction;
- yarn path is approximately sinusoidal;
- no friction between yarns;
- yarns are pinned together at the crossover points;
- negligible compressive stiffness in the yarn axial directions;
- tensile and shear responses in the non-orthogonal material coordinates are decoupled, which was verified experimentally in [16].

Under these assumptions, the micromechanical analysis of a yarn and a unit cell is carried out. Combining the simple and conventional analytical technique, the equivalent material properties used in the non-orthogonal constitutive model can be determined by the geometry and material properties of the constituents and the fabric architecture, not only by experimental data as shown in our previous paper [1].

In addition to the advantages of our non-orthogonal model developed in [1], such as accurately capturing material response under different loading conditions, the present integrated model correlates the micromechanical and microstructural parameters to the equivalent material properties used in our phenomenological constitutive equation. This model is able to reflect the complex redistribution and reorientation of fibers in the composite and account for material non-linearity and geometric non-linearity. With that, we can study the effects of various parameters on the behavior of woven composites, efficiently design the weave architecture and tailor the constituents of a woven composite for a specific application.

The shear stiffness of woven composites is closely related to the material properties of composite consti-

tuents and the architecture of woven fabric. It can be concluded that:

- Shear stiffness of the woven composite is proportional to the Young's modulus of the reinforcing fiber.
- Increasing fiber packing fraction and Young's modulus of the reinforced fibers will increase the shear stiffness of woven composites.
- Smaller inter-yarn gap sizes will result in a higher shear stiffness of woven composites because it will introduce the shear locking at an earlier stage.

Acknowledgment

Financial support from the National Science Foundation (Grant No. DMI-9900185) and Ford Motor Company are greatly appreciated.

References

- [1] Xue P, Peng XQ, Cao J. A non-orthogonal constitutive model for characterizing woven composite. *Compos Part A—Appl Sci Manuf* 2003;34(2):183–93.
- [2] Boisse P, Borr M, Cherouat A. Finite element simulation of textile composite forming including the biaxial fabric behavior. *Compos Part B: Engineering* 1997;28B(4):453–64.
- [3] Kollegal MG, Sridharan S. Strength prediction of plain woven fabrics. *J Compos Mater* 2000;34(3):240–57.
- [4] Hsiao SW, Kikuchi N. Numerical analysis and optimal design of composite thermoforming process. *Comp Meth Appl Mech Eng* 1999;177:1–34.
- [5] Peng XQ, Cao J. A dual homogenization and finite element approach for material characterization of textile composites. *Compos Part B* 2002;33(1):45–56.
- [6] Shang ZS, Suong VH. Three dimensional micro-mechanical modeling of woven fabric composites. *J Compos Mater* 2001; 35(19):1701–29.
- [7] Wang TM, Daniel IM, Gotro JT. Thermoviscoelastic analysis of residual stresses and warpage in composite laminates. *J Compos Mater* 1992;26(6):883–99.
- [8] Realf MI, Boyce MC, Backer S. A micromechanical model of the tensile behavior of woven fabric. *Textile Res J* 1997;67(6): 445–59.
- [9] Blanlot R, Billoët JL. Numerical formulation of the evolution anisotropic behavior of composite fabrics in order to simulation forming processes. In: Proceedings of ICCM-10, vol. III, Whistler, BC, Canada, August, 1995. p. 229–36.
- [10] Vu-Khanh T, Liu B. Prediction of fiber rearrangements and thermal expansion behavior of deformed woven-fabric laminates. *Compos Sci Technol* 1995;53(2):183–91.
- [11] Harrison P, Clifford MJ, Long AC, Rudd CD. A micro-mechanical approach to stress-prediction during shear for woven continuous fiber-reinforced impregnated composites. In: Proceedings of the 5th International ESAFORM Conference on Material Forming, Krakow, April 14–17, 2002. p. 275–8.
- [12] McBride TM, Chen J. Unit-cell geometry in plain-weave fabrics during shear deformations. *Compos Sci Technol* 1997;57(3): 345–51.

- [13] Bulusu A, Chen J. Shear deformation and unit cell modeling of woven fabrics using cubic spline interpolation, In: Proceedings of the 32nd International SAMPE Technical Conference, Boston, MA, November 5–9, 2000. p. 161–72.
- [14] Yu WR, Zampaloni M, Pourboghrat F, Chung K, Kang TJ. Sheet hydroforming of woven FRT composites: non-orthogonal constitutive equation considering shear stiffness and undulation of woven structure. *Compos Struct* 2003;6:353–62.
- [15] McBride TM. The large deformation behavior of woven fabric and microstructural on formed textile composite. PhD thesis, Department of Aerospace and Mechanical Engineering, Boston University, 1997.
- [16] Gutowski T. A resin flow/fiber deformation model for composites. *SAMPE Quart* 1985;16(4):58–64.
- [17] Buet-Gautier K, Boisse P. Experimental analysis and modeling of biaxial mechanical behavior of woven composite reinforcements. *Exper Mech* 2001;41(3):260–9.
- [18] Naniel IM, Ishai O. *Engineering mechanics of composite materials*. Oxford, New York: Oxford University Press; 1994.
- [19] Agarwal BD, Broutman LJ. *Analysis and performance of fiber composites*. New York, 1990 [Chapter 3].
- [20] Chen J, Lussier DS, Cao J, Peng XQ. Materials characterization methods and material models for stamping of plain woven composites. *Int J Form Process*, in press.